Int. J. Heat Mass Transfer. Vol. 15, pp. 2595–2610. Pergamon Press 1972. Printed in Great Britain

RADIATIVE HEAT TRANSFER BY FLOWING MULTIPHASE MEDIUM—PART II. AN ANALYSIS ON HEAT TRANSFER OF LAMINAR FLOW IN AN ENTRANCE REGION OF CIRCULAR TUBE

RYOZO ECHIGO, SHU HASEGAWA and HIROSHI TAMEHIRO
Department of Nuclear Engineering. Kyushu University. Fukuoka. Japan

(*Received* 20 *September* 1971)

Abstract— An analysis has been performed on the heat transfer with thermal radiation by flowing gaseous suspensions of solid and/or liquid fine particles in an inlet section of circular tube. The examination of the results on temperature profiles of both phases and heat transfer parameters illustrates that the multiphase medium is pertinent to heat transfer at high and extremely high temperatures because of the absorption behavior of the dispersed phase for thermal radiation and the results are summarized for wide ranges of parameters such as loading ratio, heat transfer characteristics between two phases, optical thickness of a duct, interaction parameter of conduction with radiation, etc. The interactions between the convection to fluid and the radiation are, thereafter, examined in some details.

NOMENCLATURE

A_p, surface area of particle $= \pi d_p^2$;
B, Planck function $= (\sigma/\pi)T^4$;
B_0, Boltzmann number $= 4\sigma T_w^4/\rho_f c_f u_{fm}$;
c_f, c_p, specific heats of fluid and particle;
d_p, particle diameter;
$F(\tau_0)$, integral defined by equation (32a);
$H(\tau_0\eta)$, integral defined by equation (11);
h_p, heat transfer coefficient between particle and fluid;
h_ξ, local heat transfer coefficient;
J, radiation intensity from the wall $= (\sigma/\pi)T_w^4$;
$K(\tau_0\eta, \tau_0\eta_1)$, integrals defined by equation (12);
k_f, thermal conductivity of fluid;
M, dimensionless parameter defined by equation (22);
N_R, radiation-conduction interaction parameter $= \kappa k_f/4\sigma T_w^3$;
Nu_d, Nusselt number of heat transfer between particle and fluid defined by equation (15);
Nu_ξ, local Nusselt number;
$Nu_{\xi,\mathrm{conv}}$, local convective Nusselt number;
$Nu_{\xi,\mathrm{rad}}$, local radiative Nusselt number;
$Nu_{\xi,\mathrm{single}}$, local Nusselt number of single gaseous phase flow;
n_p, particle concentration (number of particles in unit volume);
Pr, Prandtl number $= \mu_f c_f/k_f$;
q_{conv}, convective heat flux;
q_{rad}, radiative heat flux;
q_{total}, total heat flux;
R pipe radius;
r, radial coordinate;
Re, Reynolds number $= 2R\rho_f u_{fm}/\mu_f$;
s, distance defined by equation (5);
T_f, T_p, temperatures of fluid and particles;
T_m, mixed mean temperature of flowing suspensions;
T_0, temperature at inlet to the heating section;
T_w, wall temperature;
U, dimensionless axial velocity $= u/u_m$;

u_f, u_p, axial velocities of fluid and particles;
V_p, volume of particle = $(\pi/6)\, d_p^3$;
x, axial coordinate.

Greek symbols

Γ, thermal loading ratio = $\rho_{dp} u_{pm} c_p / \rho_f u_{fm} c_f$;
γ, loading ratio = $\rho_{dp} u_{pm} / \rho_f u_{fm}$;
ϵ_p, surface emissivity of particle;
η, dimensionless radial coordinate = r/R;
Θ, normalized dimensionless temperature = $(\theta - \theta_0)/(\theta_w - \theta_0)$;
θ_m, dimensionless mixed mean temperature of flowing suspensions defined by equation (38);
θ_{fm}, θ_{pm}, dimensionless mixed mean temperatures of fluid and particles defined by equations (36) and (37);
θ_0, dimensionless inlet temperature;
θ_w, dimensionless wall temperature (= unity);
ϕ, azimuthal angle shown in Fig. 1;
κ, absorption coefficient of particles;
μ_f, viscosity of fluid;
ξ, dimensionless axial coordinate = $(x/R)/(RePr)$;
ρ_{dp}, apparent density of dispersed medium = $\frac{1}{6}\pi d_p^3 n_p \rho_p$;
ρ_f, ρ_p, densities of fluid and particle;
σ, Stefan–Boltzmann constant;
τ, optical thickness;
τ_0, optical radius = κR.

Suffixes

conv, convection;
dp, dispersed phase;
f, fluid;
m, mean value;
o, inlet;
p, particle;
rad, radiation;
w, wall;
1, dummy variable.

1. INTRODUCTION

THE PRESENT study deals with the heat transfer by flowing multiphase medium at high or extremely high temperatures where the medium consists of the gaseous suspensions of solid and/or liquid fine particles. In the former report (Part I) [1] an analysis was performed concerning the hydrodynamically and geometrically simple laminar flow heat transfer between parallel flat plates by taking into account of thermal radiation. The results indicated that the multiphase medium exhibited a prominent perspective in the radiative heat transfer at high or extremely high temperatures and at high heat fluxes as well as the remarkable features [2–4], that is, the multiphase flow had been considered to be applicable to the convective heat transfer with high heat flux due to the increment of heat capacity and, further, might facilitate the heat transfer processes relating to the behaviors of the particulate phase. Namely the fluid temperature gradient becomes steeper in close proximity to the heating surface in spite of radiation contribution, that is attributed to the presence of fine particles (increment of heat capacity and no conductive transfer of heat among the particulate phase), while in the central core of a duct the fine particles, which absorb thermal radiation, increase not only the temperature of the surrounding carrier fluid by conduction and convection but also the mixed mean temperature and, in consequence, the Nusselt number

$$Nu_{\xi,\,\mathrm{conv}} = 2(\partial\theta_f/\partial\eta)_{\eta=1}/(\theta_w - \theta_m)$$

which characterizes the heat transfer to the fluid, increases cumulatively. Although the heat transfer mechanism is complicated by the presence of particles and radiation, the principal heat transfer mechanism may be considered as follows; for the appropriate optical radius τ_0 fine particles in the central part, which absorb

radiation, increase the surrounding fluid temperature. In single phase flow of a gas, even radiating gas the absorption coefficient is generally small, so that it is required to increase the optical length by pressurizing the gas or enlarging the hydraulic radius in order to get the high heat transfer coefficient for radiation, which yields increased power for the circulation of the medium. Since the channel dimension must be minimized for practical facilities such as nuclear reactor, heat exchanger and so on, it is rather difficult to improve the radiative heat transfer characteristics by single phase flow of gas. Actually though the infrared-inactive gases (such as He, N_2, etc.) have been frequently used because of the stable nature at high temperature they cannot contribute to thermal radiative heat transfer even at high temperature. However, it is easy to vary the optical thickness in a suspension flow system by varying the loading ratio (mass flow of fine particles to the carrier fluid), the mean size of particles with the same loading ratio, or the kind of particle materials (surface emissivity of particle: ϵ_p) without the changes of pressure and pipe radius, and these facts stimulate the practical applications eventually.

In this paper an analysis has been carried out on pipe flow of practical importance corresponding to our experimental work now under preparation. Besides as the similarity between radiative and convective transports is not valid one cannot immediately deduce the heat transfer result in a circular tube from that between flat plates. Additionally the analytical difficulty of the derivation of radiative heat flux restricts the applicable range of parameters in numerical calculations. The numerical results obtained with pipe flow are substantially rather different from those of flow between parallel flat plates. Alternatively the interaction effect of thermal radiation with convective heat transfer has been examined briefly.

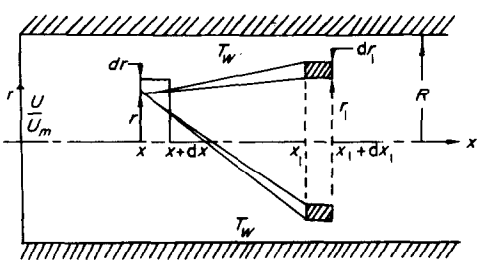

FIG. 1. Cylindrical coordinate system.

2. THEORETICAL ANALYSIS

2.1 *Description of the problem*

An analytical model employed here is shown in Fig. 1, where the coupled radiative and laminar-convective heat transfer by a gaseous suspension of fine particles in the entrance region of a pipe is considered. The basic assumptions needed for the analysis are as follows.

(i) The pipe wall is isothermal (T_w = const) and black for thermal radiation.

(ii) The flow field for both phases is fully developed and has a laminar (parabolic) velocity distribution at the pipe inlet. Both particles and fluid are at the same temperature at the inlet.

(iii) The physical properties (such as ρ, c, μ, k etc.) are constant.

(iv) The particles are spheres of uniform size and the thermal conductivity of which is large enough to neglect radial variation of temperature within the sphere.

(v) The particles are uniformly dispersed throughout the pipe cross section, and emit and absorb radiation as a grey medium in local thermodynamic equilibrium, but do not scatter. The gas is transparent for radiation.

(vi) The particles are sufficiently small and numerous to be described as a continuum for both radiation and hydrodynamics.

(vii) The presence of particles has no effect on the velocity profile of the gas.

(viii) Agglomeration or chemical reaction of particles is not considered.

(ix) The energy transports by collisions among particles or with the wall are negligible compared with those by conduction, radiation etc.

2.2 *The basic equations and their numerical method*

On the assumption that the solid particles are sufficiently small and numerous to be described as a continuum and the flow field is a fully developed (parabolic) laminar flow (but the mean velocities of the fluid and particles are not always equal), a heat balance in pipe flow yields the basic equations governing the temperature field. For the gaseous phase

$$c_f \rho_f u_f \frac{\partial T_f}{\partial x} + n_p h_p A_p (T_f - T_p) = k_f \frac{1}{r}\frac{\partial}{\partial r}\left(r \frac{\partial T_f}{\partial r}\right) \quad (1)$$

and for the dispersed phase

$$c_p \rho_{dp} u_p \frac{\partial T_p}{\partial x} + n_p h_p A_p (T_p - T_f) = -\operatorname{div} \boldsymbol{q}^R \quad (2)$$

where subscripts f and p correspond to the fluid and particulate phases, respectively and dp implies the dispersed phase. ρ_{dp} which denotes the apparent density of the dispersed phase is assumed to be constant everywhere and related to the density ρ_p with the following equation.

$$\rho_{dp} = \rho_p n_p V_p. \quad (3)$$

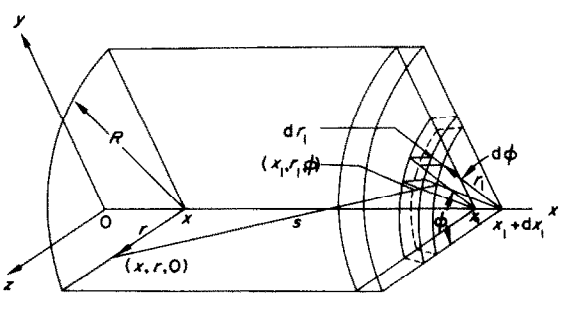

FIG. 2. Geometrical configuration for radiative heat flux.

Let us consider the cylindrical coordinate system in Fig. 2 to calculate the radiative heat flux. Noting the view factor between $(x, r, 0)$ and (x_1, r_1, ϕ) and assuming the system under study to be in thermodynamic equilibrium, the divergence of the radiative flux vector becomes

$$-\operatorname{div} \boldsymbol{q}^R = \kappa J \int_{-\infty}^{+\infty}\int_{0}^{2\pi} e^{-\tau(s_w)}(R - r\cos\phi)\, R\frac{d\phi dx_1}{s_w^3} + \kappa^2 \int_0^R Br_1 \int_{-\infty}^{+\infty}\int_0^{2\pi} e^{-\tau(s)}\, d\phi\, dr_1 \frac{dx_1}{s^2} - 4\pi\kappa B \quad (4)$$

where from Fig. 2 the distance s is given by

$$s = \{(x_1 - x)^2 + r^2 + r_1^2 - 2rr_1\cos\phi\}^{\frac{1}{2}} \quad (5)$$

s_w denotes the value of s when $r_1 = R$. In the derivation of equation (4), the radiative heat flux is approximated by one dimensional as is widely used in radiation problems, based on the assumption that radiative heat transfer in the axial direction can be neglected in comparison with radial radiative heat transfer

$$\frac{\partial q_x^R}{\partial x} \ll \frac{1}{r}\frac{\partial}{\partial r}(r q_r^R)$$

J is the radiation intensity at the wall, B is the Planck function and $\tau(s)$ is the optical thickness defined by $\tau(s) = \int_0^s \kappa(s_1) ds_1$. From geometrical consideration κ is given by the cross section of particle for radiation

$$\kappa = \pi \left(\frac{d_p}{2}\right)^2 n_p c_p. \quad (6)$$

The velocity profiles which are assumed to be equal for both fluid and particles are given by,

$$U = \frac{u_p}{u_{pm}} = \frac{u_f}{u_{fm}} = 2\left[1 - \left(\frac{r}{R}\right)^2\right]. \quad (7)$$

For brevity the boundary conditions are taken as follows

$$\left.\begin{aligned} &r = R: T_f = T_p = T_w \\ &r = 0: \partial T_f/\partial r = \partial T_p/\partial r = 0 \\ &x = 0: T_f = T_p = T_o. \end{aligned}\right\} \quad (8)$$

Strictly speaking, however, the temperature discontinuity between the heating wall and the

dispersed phase has to be examined due to the absence of the conduction term in equation (2). The results obtained with conditions equation (8) underestimate the temperature gradients in the vicinity of the wall compared with those obtained with the so-called "Radiation slip" condition [5], so that the heat transfer characteristics are also underestimated. Transforming equation (4) according to Heaslet and Warming [6] and introducing the following dimensionless variables, equations (1) and (2) are rewritten.

$$\Gamma(1-\eta^2)\frac{\partial\theta_p}{\partial\xi}+Nu_d\frac{4\tau_0^2}{\kappa d_p c_p}(\theta_p-\theta_f)$$
$$=\frac{\tau_0^3}{N_R}H(\tau_0\eta)\theta_w^4+\frac{\tau_0^4}{N_R}\int_0^1 K(\tau_0\eta,\tau_0\eta_1)\eta_1\,\theta_p^4\,d\eta_1$$
$$-\frac{\tau_0^2}{N_R}\theta_p^4 \qquad (9)$$

$$(1-\eta^2)\frac{\partial\theta_f}{\partial\xi}+Nu_d\frac{4\tau_0^2}{\kappa d_p c_p}(\theta_f-\theta_p)$$
$$=\frac{1}{\eta}\frac{\partial}{\partial\eta}\left(\eta\frac{\partial\theta_f}{\partial\eta}\right) \qquad (10)$$

where

$$H(\tau_0\eta)=\int_1^\infty K_1(\tau_0 y)I_0(\tau_0\eta y)\frac{dy}{y} \qquad (11)$$

$$\left.\begin{aligned}K(\tau_0\eta,\tau_0\eta_1)&=\int_1^\infty K_0(\tau_0\eta y)I_0(\tau_0\eta_1 y)dy\\&\qquad(\text{for }\eta>\eta_1)\\&=\int_1^\infty K_0(\tau_0\eta_1 y)I_0(\tau_0\eta y)dy\\&\qquad(\text{for }\eta_1>\eta).\end{aligned}\right\} \qquad (12)$$

I_n and K_n are modified Bessel function of the first and second kind of n-th order, respectively.

$$\gamma=\frac{\rho_{dp}u_{pm}}{\rho_f u_{fm}} \qquad (13)$$

$$Nu_d=\frac{h_p d_p}{k_f} \qquad (14)$$

$$\tau_0=\kappa R \qquad (15)$$

$$\Gamma=\frac{\rho_{dp}u_{pm}c_p}{\rho_f u_{fm}c_f} \qquad (16)$$

$$N_R=\frac{\kappa k_f}{4\sigma T_w^3} \qquad (17)$$

γ is called the loading ratio and denotes the mass flow ratio of particles to the fluid. Γ designates the flowing heat capacity ratio of two phases and it is tentatively defined as the "thermal loading ratio". γ is a convenient parameter in hydrodynamical suspension flow systems such as particulate conveyance etc., while Γ is rather convenient in heat transfer problems. The numerical value of c_p/c_f of many important materials, in practice, is of 0(1), so it may be often reasonable to put $\gamma\approx\Gamma$. Nu_d is the Nusselt number based on the diameter of particle and represents the heat transfer characteristics between a particle and the surrounding gas, which is influenced by many factors such as flow regime (laminar or turbulent flow), the occurrence of phase shifts and external forces (such as electromagnetic or sound wave field). But Nu_d approaches to the limited value 2 asymptotically as the relative velocity between two phases diminishes provided that phase shifts and external forces do not exist. N_R and τ_0 are the dimensionless parameters which denote the heat transfer ratio of conduction to radiation and the optical radius, respectively. The boundary conditions are rewritten as the following dimensionless forms.

$$\eta=1:\theta_p=\theta_f=\theta_w$$
$$\eta=0:\frac{\partial\theta^p}{\partial\eta}=\frac{\partial\theta^f}{\partial\eta}=0 \qquad (18)$$
$$\xi=0:\theta_p=\theta_f=\theta_0.$$

Equations (9) and (10) constitute simultaneous integrodifferential equations with high order of nonlinearity and it seems to be difficult to get analytical solutions. The form of basic equations is all the same as that of flow between parallel flat plates discussed in the former report [1]

except the differences of radiative heat flux and conduction term due to the use of the cylindrical coordinate system. Therefore regarding equations (9) and (10) as parabolic partial differential equation or its modified form, we calculate them numerically as the progressive type of problems by using the implicit finite difference method. Considering the equally spaced lattices in the radial direction as illustrated in Fig. 3 and assuming the i-surface

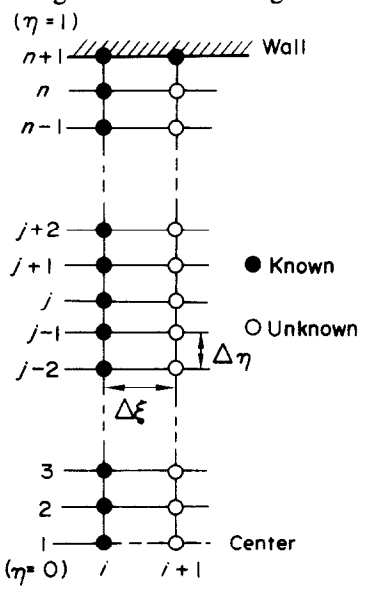

FIG. 3. Lattices of finite difference.

temperature to be known and the $(i+1)$- surface temperature unknown, the derivatives in equations (9) and (10) can be then expressed by the following finite difference approximations.

$$\left.\begin{aligned}
\frac{\partial\theta_p}{\partial\xi} &= \frac{\theta^p_{i+1,j} - \theta^p_{i,j}}{\Delta\xi} \\
\frac{\partial\theta_f}{\partial\xi} &= \frac{\theta^f_{i+1,j} - \theta^f_{i,j}}{\Delta\xi} \\
\frac{\partial\theta_f}{\partial\eta} &= \frac{\theta^f_{i+1,j+1} - \theta^f_{i+1,j-1}}{2\Delta\eta} \\
\frac{\partial^2\theta_f}{\partial\eta^2} &= \frac{\theta^f_{i+1,j+1} - 2\theta^f_{i+1,j} + \theta^f_{i+1,j-1}}{\Delta\eta^2}.
\end{aligned}\right\} \quad (19)$$

The substitution of (19) into (10), the approximation of integrals by trapezoidal formula and the replacement of $\theta^p_{i+1,j}$ in integral terms of radiative heat flux in (9) with $\theta^p_{i,j}$ as the 0-th order approximation yield,

$$\begin{aligned}
&\Gamma(1-\eta_j^2)\frac{\theta^p_{i+1,j} - \theta^p_{i,j}}{\Delta\xi} + M(\theta^p_{i+1,j} - \theta^f_{i+1,j}) \\
&= \frac{\tau_0^3}{N_R} H(\tau_0\eta_j)\,\theta_w^4 + \frac{\tau_0^4}{N_R}\frac{\Delta\eta}{2}\Big[K(\tau_0\eta_j, \tau_0\eta_1)\,\eta_1\,\theta^{p\,4}_{i,j} \\
&\quad + K(\tau_0\eta_j, \tau_0\eta_{n+1})\,\eta_{n+1}\,\theta^{p\,4}_{n+1} \\
&\quad + 2\sum_{k=2}^{j-1} K(\tau_0\eta_j, \tau_0\eta_k)\,\eta_k\,\theta^{p\,4}_{i,k} \\
&\quad + 2\sum_{k=j+1}^{n} K(\tau_0\eta_j, \tau_0\eta_k)\,\eta_k\,\theta^{p\,4}_{i,k}\Big] - \frac{\tau_0^2}{N_R}\theta^{p\,4}_{i,j} \qquad (20)
\end{aligned}$$

$$\begin{aligned}
&(1-\eta_j^2)\frac{\theta^f_{i+1,j} - \theta^f_{i,j}}{\Delta\xi} + M(\theta^f_{i+1,j} - \theta^p_{i+1,j}) \\
&= \frac{\theta^f_{i+1,j+1} - 2\theta^f_{i+1,j} + \theta^f_{i+1,j-1}}{\Delta\eta^2} \\
&\quad + \frac{1}{2\eta_j}\frac{\theta^f_{i+1,j+1} - \theta^f_{i+1,j-1}}{\Delta\eta} \qquad (21)
\end{aligned}$$

where M is the dimensionless parameter which denotes the heat transfer characteristics between particles and the surrounding fluid

$$\begin{aligned}
M &= Nu_d\frac{n_p A_p R^2}{d_p} = Nu_d\frac{4\tau_0^2}{\kappa d_p \epsilon_p} \\
&= Nu_d\frac{2\tau_0^2}{\gamma(\rho_f/\rho_p)\epsilon_p^2}. \qquad (22)
\end{aligned}$$

η_1 and η_{n+1} in equation (20) are equal to zero and unity respectively. Since equations (20) and (21) yield first order simultaneous equations of $2n$-dimensions $(\theta^f_{i+1,j},\ \theta^p_{i+1,j};\ j = 1 \sim n)$ with the same number of unknowns at the arbitrary cross section $(i+1)$, one can get solutions immediately. After obtaining $\theta^f_{i+1,j}$, $\theta^p_{i+1,j}$ $(j = 1 \sim n)$, these values are again substituted for $\theta^p_{i,j}$ $(j = 1 \sim n)$ on the right side of (21) as the 1-st order approximation. Then the similar computations are performed repeatedly until the prescribed convergence is satisfied. Advancing ξ to the next step $\xi + \Delta\xi$, the similar

iterative calculations are repeated. For actual calculation η is divided into 25 equally spaced intervals and the lattice interval along ξ is so selected that the convergence can be satisfied with several iterations. In all calculations the convergent condition is given by the following inequality.

$$\theta_{i+1,j}^{(k)} - \theta_{i+1,j}^{(k-1)} < 0{\cdot}001 \tag{23}$$

where the superscript k in the parenthesis denotes the k-th order approximation. The ranges of dimensionless parameters covered here are as follows

$$\begin{aligned} \Gamma &= 0{\cdot}1 - 10{\cdot}0 \\ M &= 0 - 4 \times 10^5 \\ N_R &= 0{\cdot}001 - \infty \\ \tau_0 &= 1{\cdot}0 - 3{\cdot}0. \end{aligned} \tag{24}$$

3. DISCUSSIONS AND RESULTS

3.1 *Dimensionless parameter*

Before examining the temperature profiles, a brief elucidation will be added to the group of parameters ξ, N_R, τ_0, Γ M introduced here

$$\xi = \frac{x}{RRePr} = \frac{(x/R)\,B_0\,N_R}{\tau_0}$$

$$\left(B_0 = \frac{4\sigma T_w^3}{\rho_f U_{fm} C_f} : \text{Boltzmann number}\right) \tag{25}$$

$$N_R = \frac{\kappa R_f}{4\sigma\, T_w^3} \tag{26}$$

$$\tau_0 = \kappa R = \left(\frac{\rho^f}{\rho_p} c_p\right)\left(\frac{R}{d_p/2}\gamma\right) \tag{27}$$

$$\Gamma = \frac{\rho_{dp} u_{pm} c_p}{\rho_f u_{fm} c_f} = \frac{c_p}{c_f}\gamma$$

$$\left(\gamma = \frac{\rho_{dp} u_{pm}}{\rho_f u_{fm}}\right) \tag{28}$$

$$M = Nu_d \frac{4\tau_0^2}{\kappa d_p c_p}. \tag{29}$$

ξ prescribes the ratio of the distance from the inlet normalized by radius R to the Péclét number of a carrier fluid as immediately found from (25) and is related to the Boltzmann number which designates the heat transfer ratio of radiation to convection, provided that R, N_R, τ_0, etc. are determined. N_R which represents the heat transfer ratio of conduction to radiation as known well, reduces to pure convective heat transfer when $N_R \to \infty$ and the radiation contribution predominates as N_R becomes smaller. However, since κ of a radiating gas is the physical property, the variation of N_R corresponds to that of the wall temperature while in a suspension flow system it should be necessary to note that κ could be artificially varied to wide extent with the diameter of particle and the concentration of it, as given in equation (6). Similarly it is easy to vary τ_0 extensively, in proportion to γ and inverse proportion to d_p without varying the channel dimension (R = const), and these two parameters have strong effects on the whole heat transfer characteristics in the radiation coupled problems as described in details in the next section. It is very important for practical applications that N_R, τ_0 in a suspension flow system can be set to the prescribed values only by changing operation conditions in a practical apparatus. It is proved theoretically that the heat transfer characteristics for a radiating gas could be improved by varying N_R, τ_0, but which is not practical. The meaning of thermal loading ratio (or loading ratio) in equation (28) is clear, however, it is not always required that the mean velocity of two phases should be equal and this is concerned with Nu_d included in M. Since it is assumed that the velocity distributions of two phases are same, the relative velocity becomes zero only in case of $u_{pm} = u_{fm}$, and then Nu_d reduces to 2.

Actually there exists a certain correlation between u_{pm}/u_{fm} and Γ (or γ) and qualitatively the former tends to decrease as the latter increases. Nu_d may be determined uniquely in laminar flow provided that $\Gamma(d_p)$ or u_{pm}/u_{fm} is given. Since the current analysis does not take into account of the various behaviors of fine

particles, the results shown here are obtained by varying Γ and M independently. Finally M depends on the total area of fine particles in unit volume as found from the coefficients of $|T_f - T_p|$ in equations (1) and (2) as well as Nu_d which indicates the heat transfer characteristics between two phases and M is related to γ and d_p. In addition, Nu_d is influenced by various body forces acting on particles (electromagnetic or sound-wave field etc.) other than u_{pm}/u_{fm}. In turbulent flow many factors have complicated effects on Nu_d.

3.2 *Temperature profiles*

The typical results of the temperature profiles calculated here are illustrated in Figs. 4–8. The

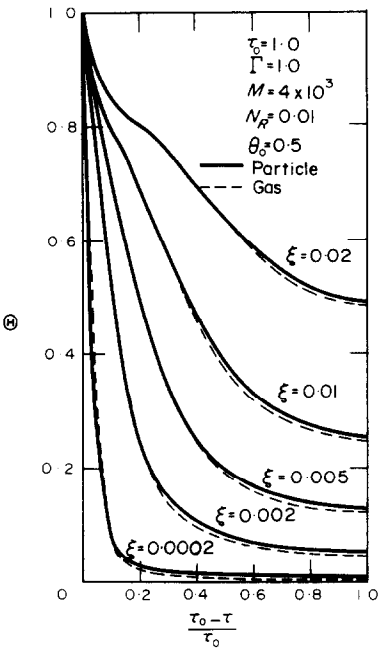

FIG. 4. Temperature profiles vs. $(\tau_0 - \tau)/\tau_0$ (effect of ξ).

ordinate and the abscissa are normalized to be $\Theta = (\theta - \theta_0)/(\theta_w - \theta_0)$, $(\tau_0 - \tau)/\tau_0$ by using dimensionless temperatures and optical thicknesses respectively and the solid and dotted curves correspond to the dispersed and fluid phases, respectively. The pronounced features

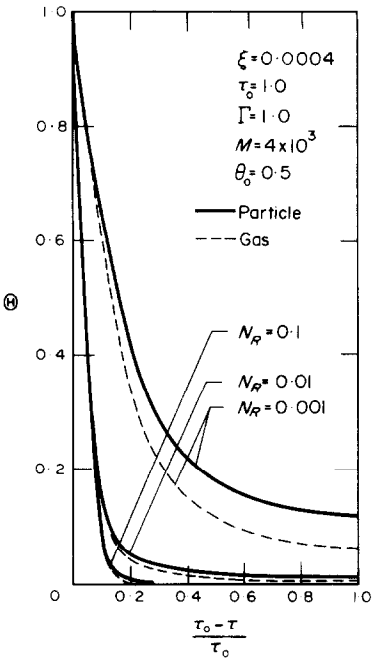

FIG. 5(a). Temperature profiles vs. $(\tau_0 - \tau)/\tau_0$ (effect of N_R).

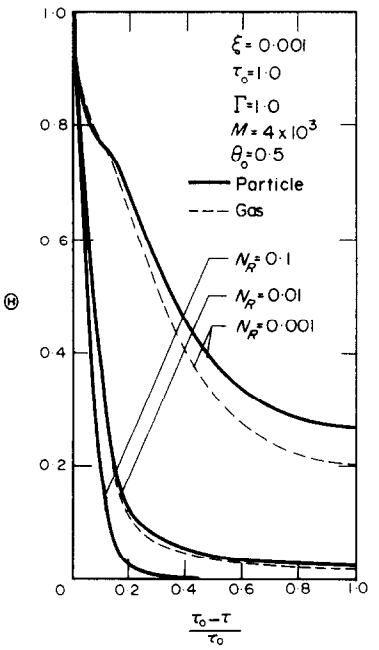

FIG. 5(b). Temperature profiles vs. $(\tau_0 - \tau)/\tau_0$ (effect of N_R).

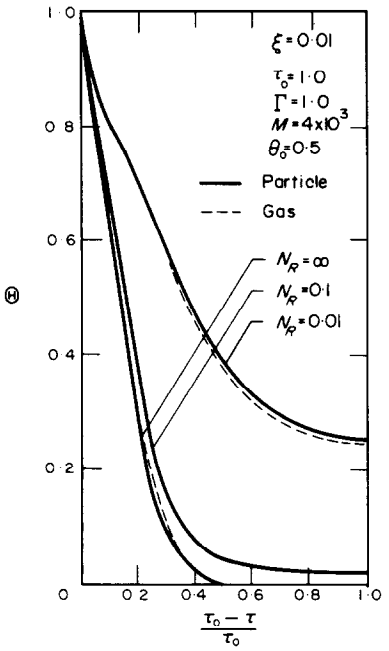

FIG. 5(c). Temperature profiles vs. $(\tau_0 - \tau)/\tau_0$ (effect of N_R).

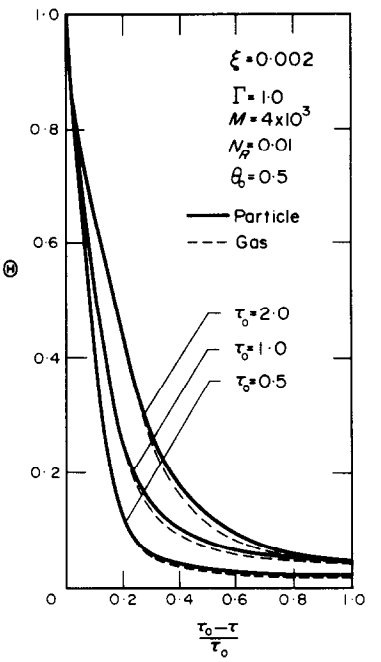

FIG. 6(b). Temperature profiles vs. $(\tau_0 - \tau)/\tau_0$ (effect of τ_0).

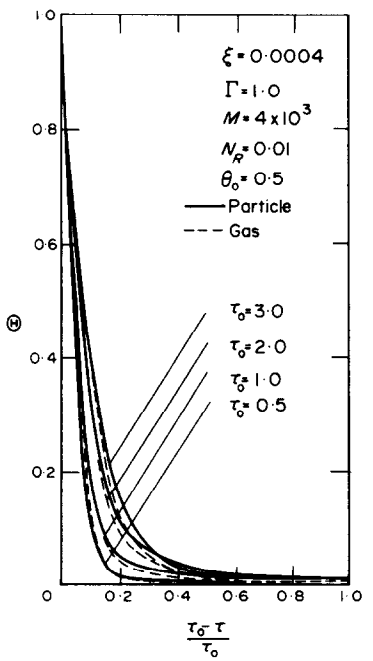

FIG. 6(a). Temperature profiles vs. $(\tau_0 - \tau)/\tau_0$ (effect of τ_0).

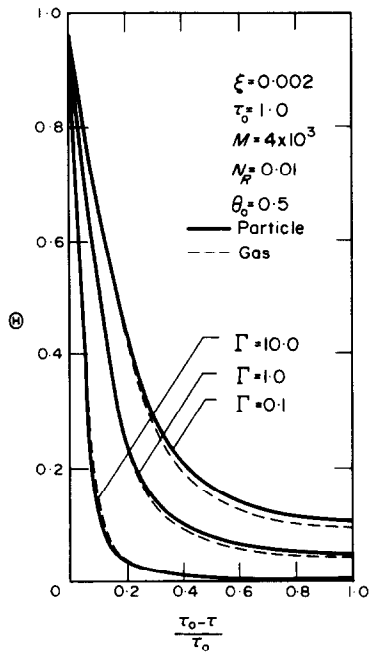

FIG. 7. Temperature profiles vs. $(\tau_0 - \tau)/\tau_0$ (effect of Γ).

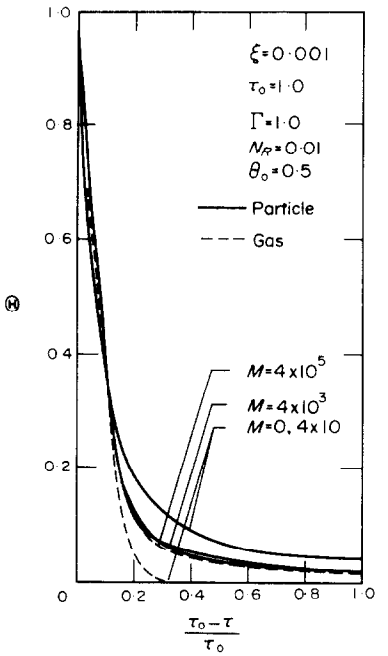

FIG. 8. Temperature profiles vs. $(\tau_0 - \tau)/\tau_0$ (effect of M).

on the temperature profiles are as follows; in the vicinity of the heating wall the temperature gradient becomes steeper for the presence of fine particles while in the central core of a pipe the fluid temperature is lifted by the heat transfer from fine particles which absorb thermal radiation, similar to the previous report. The temperature profiles have two inflection points at relatively large ξ, and for extremely small N_R even though ξ is not so large. Such a tendency is ambiguous in flow between parallel flat plates which qualitatively has the analogous temperature profile to that of single phase flow of a radiating gas [7]. However the large difference from the single phase flow is that the temperature gradient becomes steeper in the vicinity of the heating wall.

Figure 4 illustrates the variation of the temperature profiles with parameter ξ. It is a matter of course that the general features discussed above appear in Fig. 4. The temperature difference between fluid and particulate phases in the center part of a pipe varies only a little with ξ, while in the vicinity of the wall (in this region $\theta^f > \theta^p$) the smaller ξ becomes, the larger its difference becomes, and the location where both temperatures become equal is almost invariable. As understood by considering the temperature profiles in connection with the radiation heat transfer mechanism, the temperatures in the center core of a pipe increase constantly in spite of the absence of their gradients. This point is considerably different from the temperature development by the ordinary convective heat transfer. In other words, the energy transport in convective heat transfer is determined by the temperature gradient inside the fluid, on the contrary in radiative heat transfer it depends on the absorption property of the medium and the temperature profiles are determined as a consequence of absorption behavior for radiation. Thus the thermal radiation energy, which penetrates into the central core, elevates the fluid and particle temperatures. Figures 5(a)–(c) which correspond to $\xi = 0{\cdot}0004$, $0{\cdot}001$ and $0{\cdot}01$, respectively illustrate the effects of parameter N_R on the temperature profiles. The temperature differences exist at small ξ (near the inlet or for large $Re{\cdot}Pr$) even though the radiation effect is sufficiently small (such as $N_R = 0{\cdot}1$) but diminish rapidly with increasing ξ. In the case $N_R = 0{\cdot}001$ where radiative heat transfer is pronouncedly predominated the considerably large temperature differences are produced and only particles compared with fluid are considerably heated, so that this is not appropriate from the view-point of effective heating of the fluid. The fluid temperatures are higher than those of particles up to the center of a pipe for large N_R (and even for small N_R ($N_R = 0{\cdot}001$) only in the close vicinity of the wall), however the location where both temperatures become equal approaches gradually to the heating wall as N_R decreases. These tendencies are prevalent for the different values of parameters such as τ_0, Γ and M. The variation of the temperature profiles with optical radius τ_0 is given in Fig. 6. Since the radiative heat

transfer characteristics considerably depend on the absorption property of the medium and τ_0 can be varied comparatively with ease in a suspension flow system as mentioned above, the examination of the effects of τ_0 on the temperature profiles is of great importance. Qualitatively speaking the radiation energy penetrates into the medium in case of small τ_0 even though the wall is kept at high temperature and emits radiation intensively, while in case of extremely large τ_0 it can not penetrate into the central core, so that the mixed mean temperature may not be elevated.

The temperature of $\tau_0 = 3$ is highest in the range of the abscissa from 0 to 0·4 in Fig. 6(a), but is lower than that of $\tau_0 = 2$ above this value and for $(\tau_0 - \tau)/\tau_0 > 5$ it is further lower than that of $\tau_0 = 1$. In Fig. 6(b) the temperature at the central core increases for the optical radius τ_0 up to unity but when $\tau_0 = 2$ the temperature rises remarkably in the vicinity of the wall, while the temperature in the central part is rather lower. Although such a tendency analogous to this is recognized in case of flow between parallel flat plates, the quantitative effect of τ_0 differs considerably. This is due to the fact that radiative heat transfer depends on geometrical configuration and that the similarity with convective heat transfer can not be realized. Consequently the optimum value of τ_0 seems to exist under the fixed conditions of other dimensionless parameters according to the individual heat transfer problems.

Figure 7 displays the variation of the temperature profiles with thermal loading ratio Γ. Here dimensionless parameters such as τ_0 etc. are kept constant and the first factor on the right side of equation (27) may be fixed provided that the kind of particle materials is determined. Therefore the condition of heavy loading ratio Γ (or γ) under the constant optical depth τ_0 can be achieved by the employment of large particles (large d_p).

Reference to Fig. 7 reveals that the temperature differences between two phases decrease as the thermal loading ratio Γ increases and diminish at about $\Gamma = 10$ even though radiation is considerably predominated ($N_R = 0{\cdot}01$).

For large Γ the development of the temperature field is decelerated by the large heat capacity of flowing suspensions and as a result thermal entry lengths are prolonged. Such a phenomenon can be easily predicted by the reason that the dispersed phase occupies the large part of heat capacity of flowing media when the thermal loading ratio Γ is large, therefore its temperature field also dominates the fluid temperature.

Figure 8 illustrates the variation of the temperature profiles with parameter M which denotes the heat transfer characteristics between two phases. The value of $M = 4 \times 10^3$ corresponds to the case of $Nu_d = 2$ for $d_p = 10\mu$. The Nusselt number Nu_d is of 0(1) when flow is laminar and the relative velocity is not so large. $Nu_d \sim 0(10^2)$ which belongs to the turbulent regime is introduced here hypothetically. When $M = 40$ (which corresponds to large d_p because $Nu_d \geqq 2$) the temperature differences between two phases are considerable but diminish when $M = 4 \times 10^5$. The mixed mean temperatures of flowing suspensions are almost equal irrespective of M. At extremely high temperature the temperature differences are still considerable even for large M and so are they for extremely small Γ. In such a case it should be necessary to increase M artificially and improve the heat transfer from particles to a carrier gas by introducing the electromagnetic field exerted on electrically charge particles or the ultrasonic wave field and so on.

3.3 *Heat transfer results*

The total, convective and radiative heat fluxes at the wall and the local Nusselt number are defined as follows.

$$q_{\text{total}} = q_{\text{conv}} + q_{\text{rad}} \tag{30}$$

$$q_{\text{conv}} \cdot \frac{R}{k_f T_w} = \left(\frac{\partial \theta_f}{\partial \eta}\right)_{\eta = 1} \tag{31}$$

$$q_{\text{rad}} \cdot \frac{R}{k_f T_w} = \frac{\tau_0^2}{N_R} F(\tau_0)\theta_w^4 - \frac{\tau_0^3}{N_R}\int_0^1 \theta_p^4 \eta_1 H(\tau_0\eta_1)\,\mathrm{d}\eta_1 \qquad (32)$$

where

$$F(\tau_0) = \int_1^\infty K_1(\tau_0 y) I_1(\tau_0 y)\frac{\mathrm{d}y}{y^2} \qquad (32a)$$

$$Nu_\xi = \frac{h\xi 2R}{k_f} = \frac{q_{\text{total}} 2R}{k_f(T_w - T_m)} = Nu_{\xi,\text{conv}} + Nu_{\xi,\text{rad}} \qquad (33)$$

and $Nu_{\xi,\text{conv}}$ and $Nu_{\xi,\text{rad}}$ are given by

$$Nu_{\xi,\text{conv}} = q_{\text{conv}} \cdot 2R/k_f(T_w - T_m) \qquad (34)$$

$$Nu_{\xi,\text{rad}} = q_{\text{rad}} \cdot 2R/k_f(T_w - T_m). \qquad (35)$$

The dimensionless mixed mean temperatures of the fluid, dispersed and both phases are

$$\theta_{fm} = \int_0^1 U\theta_f \eta\,\mathrm{d}\eta \Big/ \int_0^1 U\eta\,\mathrm{d}\eta \qquad (36)$$

$$\theta_{pm} = \int_0^1 U\theta_p \eta\,\mathrm{d}\eta \Big/ \int_0^1 U\eta\,\mathrm{d}\eta \qquad (37)$$

$$\theta_m = \int_0^1 (\theta_f + \Gamma\theta_p) U\eta\,\mathrm{d}\eta/(1+\Gamma)\int_0^1 U\eta\,\mathrm{d}\eta \qquad (38)$$

respectively.

Equations (34) and (35) can be then rewritten.

$$Nu_{\xi,\text{conv}} = 2\left(\frac{\partial\theta_f}{\partial\eta}\right)_{\eta=1}/(\theta_w - \theta_m)$$

$$Nu_{\xi,\text{rad}} = 2\left(\frac{\tau_0^2}{N_R}F(\tau_0)\theta_w^4 - \frac{\tau_0^3}{N_R}\int_0^1 \theta_p^4\eta_1 H(\tau_0\eta_1)\,\mathrm{d}\eta_1\right)/(\theta_w - \theta_m). \qquad (39)$$

Taking notice of the heat transfer from the wall to the carrier fluid and employing θ_{fm} instead of θ_m in (39). One gets the another Nusselt number

$$Nu'_{\xi,\text{conv}} = 2\left(\frac{\partial\theta_f}{\partial\eta}\right)_{\eta=1}/(\theta_w + \theta_{fm}). \qquad (40)$$

Equations (39) and (40) do not differ from each other practically when N_R is larger than about 0·01 but they often differ considerably in case of $N_R = 0{\cdot}001$ (extremely high temperature) or extremely small Γ. Although both (39) and (40) do not precisely express the heat transfer characteristics to the carrier fluid, one can discuss them by examining these two parameters. Figure 9 illustrates the relations between Nu_ξ, $Nu_{\xi,\text{conv}}$ and ξ for the typical values of parameters τ_0, N_R and Γ. The qualitative tendency is analogous to the case of flow between parallel flat plates; that is, Nu_ξ decreases to a certain minimum and turns to increase beyond this point. This behavior implies that there exists no asymptotic Nusselt number, in other words, the temperature field can not be fully developed even in a down stream. It may be very interesting to consider this in connection with the configurations of the temperature profiles shown in Fig. 4. Nu_ξ rapidly increases and the minimum of it moves toward small ξ as N_R becomes smaller, because the temperature field develops rapidly with decreasing N_R. However $Nu_{\xi,\text{conv}}$ rather decreases in the range of small ξ. The effect of τ_0 is also considerable and similar to that of N_R, but there is almost no difference between the results of $\tau_0 = 2$ and $\tau_0 = 3$. The increasing rates of the mixed mean temperatures against ξ in Fig. 10 do not appreciably differ from each other. The effects of Γ are almost invariable on Nu_ξ in the wide range of Γ from 0·1 to 10, but vary considerably on $Nu_{\xi,\text{conv}}$.

Figure 10 illustrates the variation of the mixed mean temperatures with parameter ξ. A dotted curve denotes single phase flow. Curves 1, 2 and 9 are lower than or almost equal to that of single phase flow because in case of curves 1, 2 the heat capacities of flowing media are twice as large as that of single gaseous phase flow and that the radiation effect is small ($N_R = 0{\cdot}1$) or

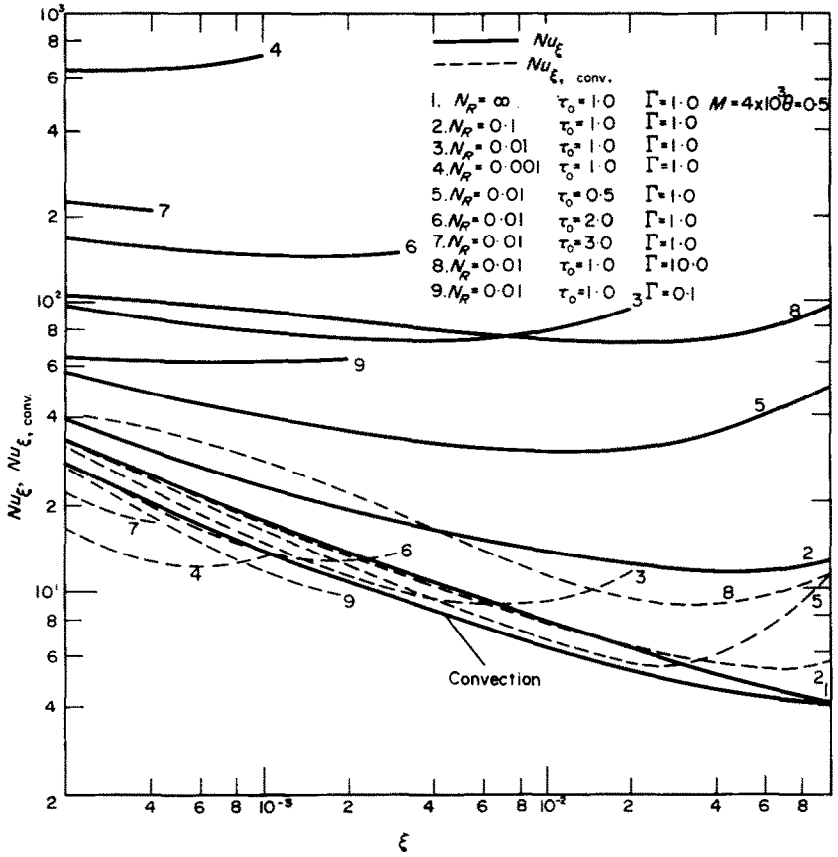

FIG. 9. Nusselt numbers Nu_ξ, $Nu_{\xi\,conv}$ vs. ξ.

zero ($N_R = \infty$), while in case of curve 9 the heat capacity is eleven times, though radiation is considerably strong ($N_R = 0{\cdot}01$). The temperature rises for various N_R, τ_0 are also found from Fig. 10. It may be necessary to examine the heat transfer characteristics in Fig. 9 together with the increasing rates of the mixed mean temperatures in Fig. 10 in the radiative heat transfer

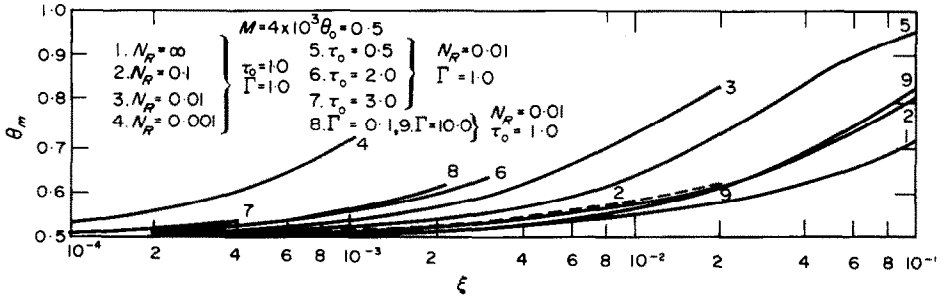

FIG. 10. Mixed mean temperatures of multiphase medium vs. ξ.

by flowing suspensions. The suspension flow system can be utilized to various kinds of applications with particular objective so that it is hard to derive the prevalent parameters which evaluate the heat transfer characteristics throughout these problems. In consequence one has to evaluate the heat transfer by examining the detailed heat transport mechanism for the particular purposes.

3.4 *Interaction effects of radiative heat transfer*

There may exist several procedures in order to estimate the interaction effects of radiation in a suspension flow system. As first procedure one can evalutate the heat transfer characteristics of the multiphase flow by comparing with that of the analytical results obtained with the hypothetical system where there is no heat exchange between two phases, from the view-point that fine particles and the carrier fluid are responsible for radiative and convective heat transfer, respectively. Secondly following to single phase flow of a radiating gas one can also discuss the interaction effects by examining the difference between the simple addition of radiative and convective heat transfer and the results taking into account of the interaction effects. Finally there exists a procedure to examine the effects of various parameters on $Nu_{\xi,\,\mathrm{conv}}$ by taking notice of the heat transfer to the fluid and considering fine particles as merely the augmentation device for heat transfer. The final procedure is employed here. Figure 11 illustrates the effects of parameter N_R. The curve $N_R = \infty$, which implies that the mass flow is twice as large as that of single phase flow ($\Gamma = 1$) shows such effects that $Nu_{\xi,\,\mathrm{conv}}$ increases by 20 per cent compared with $Nu_{\xi,\,\mathrm{single}}$ and is almost constant independently of ξ. When $N_R = 0{\cdot}1$, $Nu_{\xi,\,\mathrm{conv}}$ is almost equal to $Nu_{\xi,\,\mathrm{rad}}$ and the radiation effects on convective heat transfer is small as is shown in Fig. 9. However $Nu_{\xi,\,\mathrm{conv}}$ becomes larger

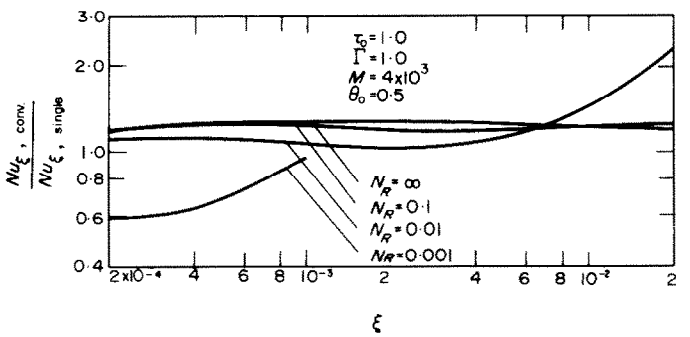

FIG. 11. Interaction effect of radiation (effect of N_R).

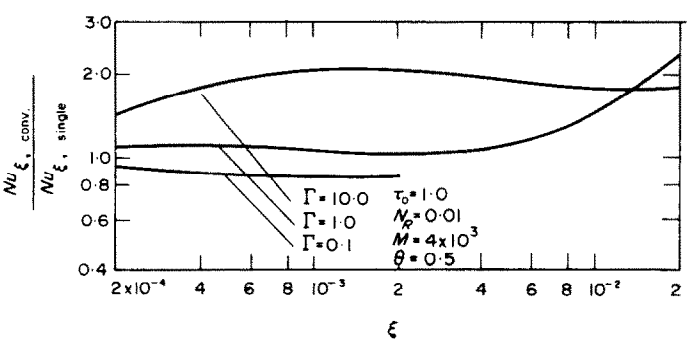

FIG. 12. Interaction effect of radiation (effect of Γ).

that that of $N_R = \infty$ as ξ increases. This implies that the relative role of radiative heat transfer, which is independent of the flow field, increases since $Nu_{\xi,\,conv}$ decreases in a down-stream when $RePr$ is fixed, while when x/R is fixed since convective heat transfer coefficient decreases due to the decrease of $RePr$. Accordingly the interaction effect on convective heat transfer by radiation increases as the radiation contribution increases or N_R becomes smaller and $Nu_{\xi,\,conv}$ with radiation exceeds that of $N_R = \infty$ without radiation at certain ξ. At extremely high temperature ($N_R = 0{\cdot}001$) convective heat transfer may be neglected compared with radiative heat transfer and reduces to about half of that in case of $N_R = \infty$ in the range of small ξ but thereafter tends to increase rapidly ($Nu_{\xi,\,conv}$ at large ξ is not calculated here). One can deduce from this fact that $Nu_{\xi,\,conv}$ may become considerably large at large ξ and thus radiation has a strong effect on convective heat transfer over the entire range of ξ. Figure 12 displays the variation of the ratio of $Nu_{\xi,\,conv}$ to $Nu_{\xi,\,single}$ with ξ when radiation is rather strong ($N_R = 0{\cdot}01$). For large Γ it considerably influences convective heat transfer but its effect is almost constant for all ξ. This is understood by considering that convective heat transfer does not change with the axial locations and the flow velocity because the major amount of heat transferred by radiation is stored in fine particles. Such a heat transfer route as "radiation → fine particles → fluid" becomes predominant as Γ decreases, so that convective heat transfer is influenced considerably.

4. CONCLUSIONS

In the current paper an analysis has been performed on the coupled radiation and laminar convective heat transfer by flowing suspensions at high or extremely high temperatures, and the various effects of parameters on the temperature and the heat transfer characteristics have been discussed in some details. The important conclusions obtained here are as follows; (1) The coupled radiation and laminar convective heat transfer in a pipe by flowing suspensions remarkably improves the heat transfer characteristics; that is, the temperature gradient becomes steeper by the presence of particles in the vicinity of the wall, while in the central core of a pipe the temperature is elevated by thermal radiation.

(2) The results obtained here are considerably different from those of flow between parallel flat plates both quantitatively and qualitatively since radiative heat transfer depends on geometrical configuration and that the similarity between convective and radiative heat transfer is not valid in this system.

(3) There is no fully developed profile in the temperature field even in a downstream; that is, the Nusselt number decreases to a certain minimum and thereafter tends to increase as ξ increases. Additionally the temperature profile deviates from that of ordinary convective heat transfer. These behaviors are considered to be connected with each other.

(4) Radiative heat transfer can not be improved for small τ_0, on the contrary for excessive large τ_0 it becomes uneffective since radiation can not penetrate into the central core. Accordingly there exists the optimum value of τ_0, which also influences other parameters. Being different from single phase flow of a radiating gas it is relatively easy to change τ_0 in a suspension flow system.

(5) In a suspension flow system several methods are thought to estimate the interaction effect of radiation. The heat transfer mechanism has been clarified by evaluating the effect on convective heat transfer.

(6) In a suspension flow system many applications are considered in its use, so that it should be necessary to examine the heat transfer mechanism by taking into account not only of the heat transfer characteristics but also of the mixed mean temperature.

REFERENCES

1. R. ECHIGO and S. HASEGAWA. Radiative heat transfer by flowing multiphase medium. Part I: An analysis on heat

transfer of laminar flow between parallel flat plates. *Int. J. Heat Mass Transfer* **15**, 2519–2534 (1972).
2. C. L. TIEN. Heat transfer by a turbulently flowing fluid–solids mixture in a pipe. *J. Heat Transfer* **83C**, 183–188 (1961).
3. L. FARBAR and M. J. MORLEY. Heat transfer to flowing gas–solids mixtures in a circular tube. *Ind. Engng. Chem.* **49**, 1143–1150 (1957).
4. C. A. DEPEW and L. FARBAR. Heat transfer to pneumatically conveyed glass particles of fixed size. *J. Heat Transfer* **85C**, 164–172 (1963).
5. R. VISKANTA. Radiation transfer and interaction of convection with radiation heat transfer. *Advances in Heat Transfer*, Vol. 3. pp. 175–251. Academic Press, New York (1966).
6. M. A. HEASLET and R. F. WARMING. Theoretical prediction of radiative transfer in a homogeneous cylindrical medium. *J. Quant. Spectrosc. Radiat. Transfer* **6**. 751–774 (1966).
7. Y. KUROSAKI. Pre-print of 795th Lecture Meeting. in Japan Society of Mechanical Engineers. pp. 13–16 (1969).

RAYONNEMENT THERMIQUE PAR UN MILIEU MULTIPHASIQUE EN ECOULEMENT—II. ETUDE DU TRANSFERT THERMIQUE D'UN ECOULEMENT LAMINAIRE DANS LA REGION D'ENTREE D'UN TUBE CIRCULAIRE

Résumé—On a conduit l'étude du rayonnement thermique par des suspensions de fines particules solides et (ou) liquides entraînées par un gaz dans la section d'entrée d'un tube circulaire.

L'examen des profils de température obtenus pour les deux phases et des paramètres de transfert thermique montre que le milieu multiphasique est sensible au transfert thermique à des températures élevées ou extrèment hautes à cause de l'absorption du rayonnement par la phase dispersée. Les résultats sont résumés pour de grands domaines de variation des paramètres tels que le rapport de charge, les caractéristiques de transfert thermique entre les deux phases, l'épaisseur optique du conduit, le paramètre d'interaction de la conduction avec le rayonnement, etc. . . . Les interactions entre la convection et le rayonnement sont étudiées en détail.

WÄRMEÜBERTRAGUNG DURCH STRAHLUNG BEI EINEM FLIESSENDEM VIELPHASEN-MEDIUM. TEIL II: EINE UNTERSUCHUNG DES WÄRMEÜBERGANGS BEI LAMINARER STRÖMUNG IM EINTRITTSGEBIET EINER KREISFÖRMIGEN RÖHRE

Zusammenfassung—Untersucht wurde der Wärmeübergang mit Temperaturstrahlung bei fliessenden gasförmigen Suspensionen von festen und/oder flüssigen kleinen Teilchen im Eintrittsgebiet einer kreisförmigen Röhre. Die Sichtung der Ergebnisse für die Temperaturprofile bei den Phasen und den Wärmeübergangskoeffizienten zeigt, dass das Vielphasenmedium für die Wärmeübertragung bei hohen und sehr hohen Temperaturen geeignet ist, wegen der Absorption von Temperaturstrahlung durch die dispergierte Phase. Die Ergebnisse sind für einen grossen Bereich von Parametern zusammengefasst wie Beladung mit Teilchen, Wärmeübergangskoeffizient zwischen zwei Phasen, optische Dicke der Leitung, Wechselwirkungsparameter der Leitung mit der Strahlung u.s.w.

Anschliessend werden die Wechselwirkungen zwischen der Konvektion in der Flüssigkeit und der Strahlung ausführlich behandelt.

ЛУЧИСТЫЙ ПЕРЕНОС ПРИ ТЕЧЕНИИ МНОГОФАЗНОЙ СРЕДЫ

ЧАСТЬ 2. Анализ теплообмена в ламинарном потоке на входном участке круглой трубы

Аннотация—Проведен анализ лучистого переноса тепла при течении газовзвесей с твердыми и жидкими мелкими частицами во входном участке круглой трубы. Анализ измеренных распределений температуры обеих фаз и параметров теплообмена показывает, что многофазная среда пригодна для теплообмена при высоких и сверхвысоких температурах благодаря абсорбционным свойствам диспергированной фазы при тепловой радиации. Результаты обобщаются для широкого диапазона таких параметров, как относительные концентрации, характеристики теплообмена между двумя фазами, оптическая толщина трубы, параметр взаимодействия излучения и теплопроводности и т.д. Взаимодействие конвекции и излучения исследованы более детально.